

Infinigen-Sim: Procedural Generation of Articulated Simulation Assets

Abhishek Joshi¹ Beining Han¹ Jack Nugent¹ Yiming Zuo¹
 Jonathan Liu¹ Hongyu Wen¹ Stamatis Alexandropoulos¹ Tao Sun^{1,2}
 Alexander Raistrick¹ Gaowen Liu³ Yi Shao¹ Jia Deng¹

¹Princeton University ²McGill University ³Cisco

Abstract:

We introduce Infinigen-Sim, a toolkit which enables users to create diverse and realistic articulated object procedural generators. These tools are composed of high-level utilities for use creating articulated assets in Blender, as well as an export pipeline to integrate the resulting assets into common robotics simulators. We demonstrate our system by creating procedural generators for 5 common articulated object categories. Experiments show that assets sampled from these generators are useful for movable object segmentation, training generalizable reinforcement learning policies, and sim-to-real transfer of imitation learning policies.

Keywords: Robot Simulation, Articulated Objects, Procedural Generation

1 Introduction

Interacting with articulated objects is an essential step in many important applications for robotics. From using hinged fridges and dishwashers, pushing buttons, opening drawers, to traversing doors with various handles, robots require the ability to manipulate articulated objects to accomplish useful tasks in the real world.

Learning in physical simulation [2, 3, 4, 5, 6, 7] has proven a useful strategy for many robotics tasks [8, 9, 10, 11, 12, 13, 14, 9]. To best use this strategy for articulated object manipulation, we require large-scale datasets of articulated assets with as great a diversity of geometry and joints as possible. Articulated assets are challenging to acquire, as objects curated from the internet [15, 16] or 3D-scanning [17] are typically static and lack joint annotations. Widely used articulated object datasets instead use labor-intensive human annotation [18, 19, 20, 21, 22] for joint position and axes, which limits the number of unique geometries and articulation annotations.

To this end, we propose Infinigen-Sim, a tool which enables the creation of diverse articulated assets through procedural generation. To complement existing sources of data, we envision that users can choose an object class of interest (e.g. lamps, doors) and create a *procedural generator* for it, which is a 3D graphics program that outputs assets of the class as a function of optionally randomized parameters (e.g. dimensions, part placement). Our approach has many advantages:

Unlimited kinematic variation: Procedural generators can sample assets with dense coverage of important physical dimensions, e.g. the handle-to-hinge distance of a door. This means interacting with the assets requires different trajectories, e.g. different radius arcs of an end effector opening doors with different handle-to-hinge distances. Continuous variation also applies to geometry detail (e.g. edge bevel radii) and tolerances (e.g. toaster slot width), which all serve to create dense coverage and diverse training data.

Combinatorial coverage: Procedural generators can randomly swap sub-parts to use different procedural generators (e.g. drastic changes in handle style: knobs, levers, crash-bars). We can also easily



Figure 1: Panels (a)-(e) show sampled assets generated using Infinigen-Sim. We develop generators for the door, toaster, refrigerator, dishwasher, and lamp categories. As shown in Panel (f), our assets are can be directly integrated within Infinigen [1] scenes to train robot policies in highly diverse, photorealistic, large-scale simulation environments.

express variable-quantity arrays of articulated parts (e.g. 1-5 fridge drawers), as well as very small parts (e.g. tiny buttons on a toaster), which be challenging for annotators or image-based capture.

Uniformly high-quality: Each procedural generator is code that can be verified for correctness. This means our joint locations and axes do not make errors for individual asset instances as can happen for human annotation. Our procedural assets also have realistic materials (derived from Infinigen Indoors) and detailed but efficient geometry with no holes or protruding triangles.

Infinigen-Sim builds on 3D-graphics and procedural generation tools from Blender [23] and Infinigen Indoors [1], but adds tools and generators designed for articulated object generation. Specifically, we augment Blender’s Geometry-Nodes system with new modules (known as *node-groups*) which implement hinged and sliding joints for procedural assets and ensure that these joints are represented in a unified format for use by downstream tools. We provide export code which converts assets created using these tools into high quality assets for simulation in popular formats such as URDF, USD, and MJCF.

Experiments show that objects created using procedural generators created with Infinigen-Sim are useful for tasks in both vision and robot learning. Specifically, we used Infinigen-Sim to create articulated procedural generators for 5 object categories, namely: doors, toasters, fridges, dishwashers and lamps (shown in Fig. 1). We use these to generate datasets for movable part segmentation and achieve better generalization for more detailed articulated parts. We also train both RL and imitation learning policies on simulation data and show improved generalization to unseen object instances and demonstrated successful sim-to-real transfer through real-world experiments on a Franka Panda robot arm.

We hope Infinigen-Sim will complement existing articulated assets by providing dense high-quality coverage for specific object classes, and we hope this library of pre-implemented object generators will grow through open-source engagement with the community.

2 Related Work

Asset Datasets for Robot Simulation. Although works have collected large-scale static 3D asset datasets [16, 15], interactive and articulated 3D datasets [18, 24, 25, 26, 22] remain limited in both quantity and quality. Sapien [18] collected 2k+ assets from PartNet [24] and manually annotated the articulated joints. Others [19, 20, 27] scanned real-world objects to curate separate articulated object datasets. However, issues like inaccurate joint annotations and a lack of kinematic diversity remain. Infinigen-Sim instead adopts a new approach (procedural generation) which has precise ground truth and is highly scalable, only requiring a new procedural generator for each object *class*, with no human time cost for each unique object geometry or articulation configuration.

Articulated Object Generation. Recent work has exploited AI techniques to augment and diversify static asset datasets [16, 28] to create articulated objects [29, 30]. However, these systems lack controllability of asset geometries and do not guarantee correct joint configurations [31]. Prior work [32, 29, 33, 34, 35, 36, 30, 37] has also generated articulated assets with real-to-sim pipelines. Paris [34] learns part-based neural radiance fields to reconstruct articulated assets. Real2Code [33] and URDFFormer [35] constructs URDFs with RGB images as input, using a mixture of off-the-shelf vision models and LLMs. That being said, real-to-sim approaches often fail to construct articulated assets with high-quality. Additionally, these methods fall short on capturing occluded articulations and tend to produce inaccurate geometries and joint annotations [31]. Inherited from Infinigen-Indoors [1], our tool allows users to model each individual part from scratch including its joint properties. This means users can also easily create high quality articulated bodies that may be occluded by outer surfaces (see Fig. 1(c) and (d)).

Procedural Generation. Many prior works create procedural training data focused on indoor environments [5, 38], nature [38] and cities [39] but do not create procedural articulated objects. More similar to our work is Eppner et al. [40], which introduces a scene generator including some procedural articulated assets made in Python. However, their assets are composed mainly of mesh primitives (cubes/cylinders), do not contain multi-level articulations (e.g. pivoting handle on a pivoting door), and is extensible only by programmers. Our system is constructed using Blender, has detailed geometry and materials, and extensible by both programmers and anyone familiar with Blender.

3 Infinigen-Sim

Infinigen-Sim is designed to aid in creating procedural generators which produce simulation-ready articulated assets. It is composed of a set of procedural articulation tools, followed by export code which produces a file for use in robotics simulators. This overall workflow is visualized in Fig. 2.

3.1 Articulation Procedural Generator Tools

Infinigen-Sim leverages Blender’s procedural modeling tools [23], especially *Geometry Nodes* and *Shader Nodes*, which are an artist-friendly, GUI-based, domain specific language for procedural generation. These tools allow users to create meshes and materials by composing primitives, geometric transformations, and scalar vector arithmetic, all represented as nodes in a direct acyclic graph. Geometry nodes are widely adopted among 3D artists in the modeling community, with extensive documentation and a large ecosystem of tutorials and resources. These node-based tools are general purpose and can represent essentially all desirable object geometries.

To design articulated assets within this system, we create two new nodes that implement revolute and prismatic joints. These nodes accept two incoming geometries (defined via prior nodes) and introduce a parent-child relationship annotated with the relevant joint type. Each joint node also al-

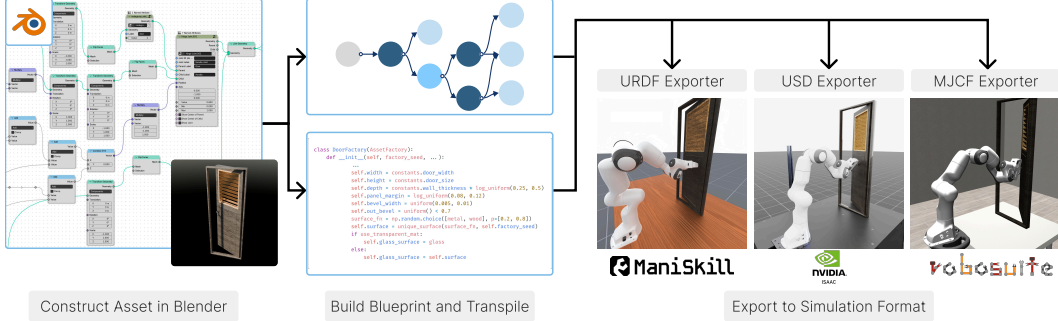


Figure 2: Users create a procedural asset using Blender’s Geometry Nodes feature and our custom joint nodes. The node graph is then converted to Python code and a corresponding blueprint storing the kinematic structure is created. We sample parameters to generate the asset and pass both the asset and blueprint to the exporter, which recursively builds a simulation-ready articulated object.

lows users to set the pivot position, axis, and joint range, either as fixed values or through parameters passed from other nodes. Users can leverage Blender’s built-in math nodes to compute these values directly from the asset’s geometry within the node graph. Several example uses of these joint nodes are shown in Appendix Sec. A.2.

These joint nodes have three purposes. First, they directly speed up the procedural generator creation process, since they implement a commonly used operation which no longer needs to be reimplemented for each object that uses a hinge or sliding joint. Second, they provide immediate visual feedback as to the effect of a joint: a hinge joint node with a certain origin or angle extent input will immediately transform the child geometry in the GUI according to those inputs, which prevents erroneous values and can be used to debug any arithmetic expressions responsible for calculating the joint parameters. Third, this standardized implementation of joints allows us to add logic to save all joint metadata in a standard format for later use.

Our joint nodes support the creation of many articulated structure types such as jointing multiple meshes together in a chain, jointing multiple meshes to one parent, and connecting two geometries via multiple joints. We also create an additional custom node group that supports duplicating jointed bodies at defined points. This can be effective for procedurally duplicating articulations such as burners on a cooktop or shelves in a dishwasher without having to manually define each joint. Examples of all these cases can be found in Appendix Sec. A.2. Our joint nodes also optionally take as arguments semantic labels for the joint and the parent and child bodies. We develop an additional custom node that users can directly inject into their graph for more fine-grained labeling of individual parts. Finally, we provide a utility script that checks if any two rigid parts of the asset penetrate each other within a defined range of motion. This helps users to adapt joint configurations and parts’ geometries to avoid self-collision and penetration problems.

3.2 Exporting Assets to Simulation

Converting procedural articulated assets from Blender to a simulation-ready format involves three steps, all of which are automated. First, given the user’s articulated object in Blender, we use the Blender Python API to parse and update the asset’s node graph. During this step, we inject Blender-provided *Store Named Attribute* nodes into the original graph. These nodes assign values for attributes to different parts of the geometry that will be beneficial later during exporting. We also create a kinematic blueprint for the object class (inspired by [41, 42]) that abstracts away the full procedural graph while preserving the essential details required for articulation. We note that a kinematic blueprint is generated for an asset category, not an individual instance.

Second, after generating a blueprint, we use Infinigen’s [38] transpiler to convert the updated node graph to Python code. Users can edit this code to customize asset parameter distributions or further tune node graph structures. Thus, our tool gives users fine-grained control over generated assets.

The final step is to export the asset into a simulation-compatible format. Using the transpiled code, we sample random parameters and construct a new instance of the asset. We then pass this geometry along with its category’s corresponding kinematic blueprint to an exporter for either one of the URDF, USD, or MJCF file formats. The exporter recursively traverses the kinematic blueprint to build the final simulation-ready asset including all joints, rigid geometries, and semantic metadata. During this process, users can generate convex-decomposed collision meshes with third-party tools like CoACD [43].

Asset Category	Discrete Variations	Continous Variations
Door	Door count: 1–2; Handle types (5): lever, knob, pullbar, crashbar, no handle; Door types (3): louver, glass, panel; Hinge sides (2): left, right.	39 dimensions
Fridge	Door count: 1–2; External drawer count: 0–2+; Internal shelf count: 0–3+; Internal drawer count: 0–2+; Number of shelves per door (4): 0–4.	32 dimensions
Dishwasher	Rack count: 0–3+; Button count: 0–6+; Button types (2): square, circle; Handle types (2): square, circle; Handle curvature (2): curved, square.	13 dimensions
Lamp	Arm segments: 0–3; Type of joint for segment (2): rotational, translational; Switch types (4): rocker, twist, push, pull-string; Switch location: base/head (n/a for pull-string).	29 dimensions
Toaster	Number of slots: 1–3+; Body protrusion axis (2): x-axis, y-axis; Levers per slot: 1–2; Types of levers (5): cylinder, half-cylinder, ellipsoid, sphere, flat; Buttons per lever: 0–3+.	14 dimensions

Table 1: Procedural articulated object generators can *densely* cover a cartesian-product of possible subcomponents and continuous parameters. For each object, we show the list of possible discrete variations (e.g. swappable sub-components) and calculate the total number of combinations of these components. We do not count material randomization. Then, we list the number of independent continuous parameters (see Appendix Sec. A.3 for names), summed over subcomponents, which specifies the *dimensionality* of the continuous parameter space. Combining discrete and continuous variations, and assuming 3 values per continuous parameter, our system can generate between 10^6 to 10^{20} unique assets per category.

4 Procedural Articulated Asset Generators

Using our custom joint and utility nodes, users can create a variety of physically accurate, kinematically diverse, photorealistic assets. We demonstrate the capabilities of Infinigen-Sim by developing procedural generators for five categories of articulated assets including doors, toasters, fridges, dishwashers, and lamps. These articulated procedural generators were created in 1–7 hours per object class by novice and intermediate Blender users, mostly dominated by time to create the static procedural asset.

Examples of assets sampled from these generators can be seen in Fig. 1. Table 1 showcases the variations we consider for each asset category. Similar assets in PartNet-Mobility [18] are quite limited in quantity.

All assets created in this way have many continuously varying input parameters, which can either be manually set or randomized according to a distribution. We show a case study for just doors with lever handles in Fig. 3. To open a door with a handle, two parameters are important for manipulation: the length of the handle and the distance between the handle hinge and the door hinge. The former defines grasp poses and the motion of handle rotation. The latter determines the trajectory required to successfully rotate the door. Infinigen-Sim allows users to define widely distributed combinations of these two parameters with diverse handle geometries. Users can tailor distributions of parameters to their specific needs. Such properties cannot be satisfied with existing articulated assets [18, 19] or modeling tools [29, 33].

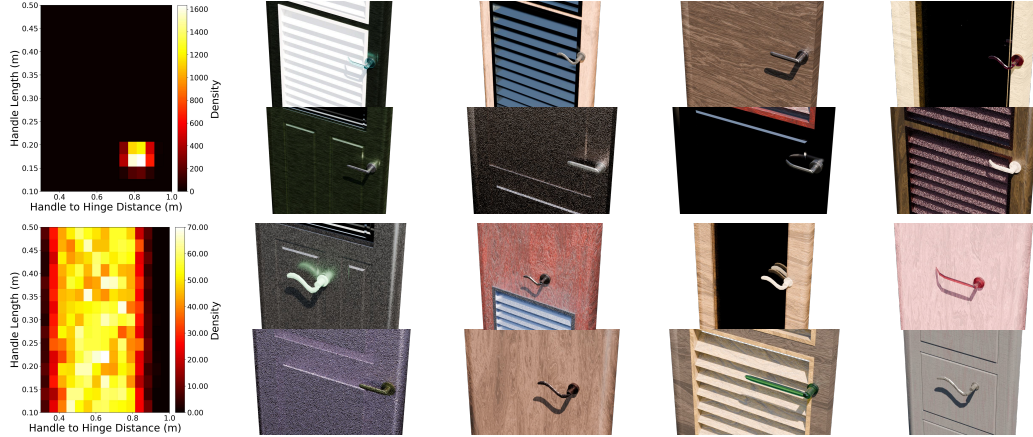


Figure 3: Comparison of asset parameter distributions. The top row shows the default distribution used for handle length and handle-to-hinge distance. The bottom row shows an expanded distribution where these parameters are varied over a wider range.

5 Experiments

We demonstrate that assets created with Infinigen-Sim help downstream vision and robot learning tasks, including movable part segmentation, RL generalization, and sim-to-real transfer.

5.1 Movable Part Segmentation

Movable part segmentation [44, 18] is an important vision task for embodied agents. Given an RGB image of an object, the model must segment each articulated part. We focus on five categories of assets including doors, toasters, refrigerators, dishwashers, and lamps. First, we generate 250 diverse assets per category using Infinigen-Sim. Then, we follow a similar setup as Xiang et al. [18] to generate image datasets for both PartNet-Mobility and Infinigen-Sim assets. We split the PartNet dataset such that images rendered from 75% of the assets are used for training and the remaining 25% are used for evaluation. All models are evaluated on images of *unseen* PartNet assets only. We finetune a pretrained Mask R-CNN model with a ResNet-50-FPN backbone, as in [45], for three datasets: 1) P15k, approximately 15k images of PartNet assets only, 2) P30k, approximately 30k images of PartNet assets only, and 3) P15k+I, a combination of approximately 15k images of PartNet assets and 15k images of Infinigen-Sim assets. Please refer to Appendix A.4 for more details on data generation and model training.

Through our experiments, we observe that doubling the size of the original dataset (P30k) yields only marginal improvements (see Appendix A.5 for overall results). This suggests the model may not be learning new features that improve generalization to unseen assets despite scaling the training images from PartNet assets alone. In contrast, adding the same number of images using Infinigen-Sim assets yields a larger performance gain. As shown in Table 2, this improvement is more significant across smaller articulated parts such as door handles, toaster levers, dishwasher buttons, and lamp switches. This suggests a core benefit of Infinigen-Sim. Namely, our tool allows users to procedurally scale articulated parts that require a greater level of detail. Achieving this level of granularity is labor-intensive for manually annotated articulation datasets.

5.2 Reinforcement Learning Generalization

We demonstrate that Infinigen-Sim assets help reinforcement learning robot policies generalize to novel object instances. We evaluate on the following tasks.

1. **Push Down Toaster Lever.** The robot is tasked with pushing down the lever of the toaster. Only toasters with a single lever are considered for this task. We evaluate on 5 unseen PartNet

	Door			Toaster				Refrigerator	
Dataset	Frame	Body	Handle	Body	Lever	Knob	Button	Body	Door
P15k	57.41	71.87	41.08	96.96	59.76	55.31	4.20	81.35	66.37
P30k	59.21	74.65	40.31	97.15	59.05	57.50	3.70	82.76	69.00
P15k+I	59.64	73.17	44.97	96.87	64.31	54.69	5.82	84.37	67.82
	Dishwasher					Lamp			
Dataset	Body	Door	Shelf	Button	Knob	Base	Rod	Head	Switch
P15K	84.23	73.32	0.13	24.59	0.00	54.75	7.27	78.09	11.45
P30k	85.14	75.14	0.21	21.31	0.00	51.72	7.22	77.86	10.45
P15k+I	86.59	75.31	0.17	31.01	0.02	55.40	7.03	77.63	17.44

Table 2: Movable part segmentation performance per articulated part type. We train a model for 50 epochs and report the evaluation mAP scores averaged across 3 seeds. Using Infinigen-Sim assets results in stronger model generalization for relatively smaller articulated parts, e.g. door handles, toaster levers, dishwasher buttons, and lamps switches.

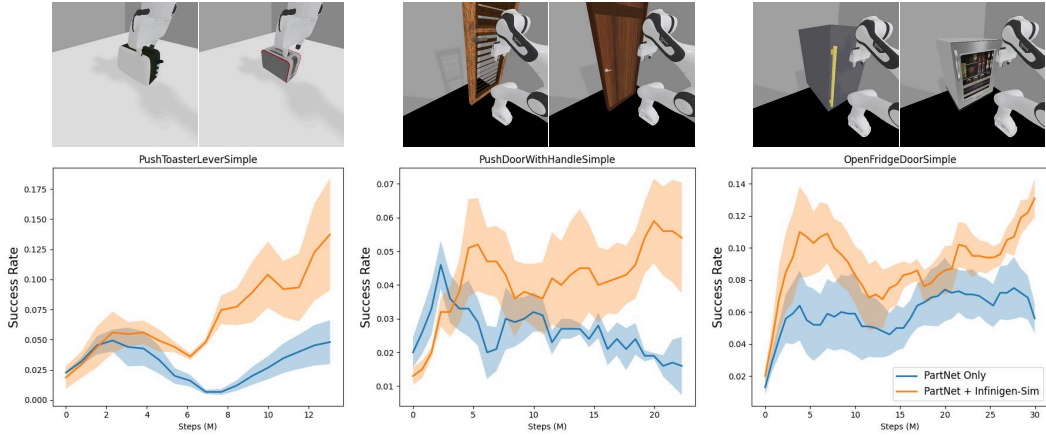


Figure 4: Top row: RL environment setup in Maniskill3 [2]. From left to right: Push Down Toaster Lever, Push Door with Handle, Open Fridge Door. Bottom row: learning curve on the testing PartNet instances for all three tasks. Each curve shows the mean and standard deviation of 4 runs.

toasters and compare RL policies where one is trained on the remaining 8 PartNet toasters while the other is trained on 8 PartNet and 14 Infinigen-Sim toasters.

2. **Push Door with Handle.** The robot needs to push the door open by first rotating the door handle clockwise by more than 40 degrees. Only single doors with a lever handle are considered for this task. We evaluate on 3 PartNet doors with handles and compare RL policies where one is trained on the remaining 3 PartNet doors while the other is trained on 3 PartNet and 44 Infinigen-Sim doors.
3. **Open Fridge Door.** The robot is tasked with grasping the handle and opening the fridge door. Only refrigerators with a single door are considered for this task. We evaluate on 5 PartNet fridges and compare RL policies where one is trained on the remaining 5 PartNet fridges while the other is trained on 5 PartNet and 44 Infinigen-Sim fridges.

We train PPO [46] policies using GPU-parallel heterogeneous simulation across 64 environments in ManiSkill3 [2]. Simulator environments using Infinigen-Sim assets ran at speeds indistinguishable from those using PartNet-Mobility. For all tasks, the policy takes as input an RGB image from a third-person view and its end-effector pose with no additional privileged information. The output at each time step is a delta pose command for operational space control (OSC). Refer to the appendix for details.

Figure 4 shows the learning curve (averaged over 4 runs) during evaluation on unseen PartNet assets. It is clear from this figure that training policies with a combination of Infinigen-Sim and PartNet assets results in better generalization than training with only PartNet assets. PartNet-Mobility assets provide limited visual and geometric diversity across these categories. Additionally, misaligned joints (e.g. an incorrect pivot position for a door handle) may make tasks harder to complete and hinder policy learning. In contrast, our tool provides dynamically accurate assets with both great visual and geometric diversity. Our assets are also able to cover a wider distribution of values for important parameters (see Figure 3) that impact a robot’s trajectory. Through these RL experiments, we claim that our tool complements existing datasets and can boost generalization capabilities to unseen model instances.

5.3 Sim-to-Real Transfer

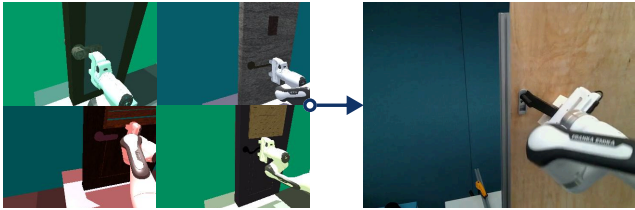


Figure 5: An imitation learning policy trained using Infinigen-Sim assets (left) achieves a 7/10 success-rate on opening a real door (right).

and filter successful ones as the demonstration dataset. The robot takes an RGB image from its on-the-shoulder camera and the end effector pose as inputs. We train ACT [48] on 1k+ trajectories with randomized lighting, joint initialization, and camera views. For comparison, we curate two datasets including one with 300+ Infinigen-Sim assets and another with all 6 PartNet assets.

We evaluate the zero-shot performance on a real world door. For each trial, we randomly initialize the robot’s pose. We observe that policies trained with Infinigen-Sim assets achieve 7 out of 10 successes in the real world, while those trained with PartNet assets fail on all 10 trials. This increase in performance is likely a result of the diversity and quantity of assets generated with our tool. These experiments show that our tool has the ability to create articulated assets diverse enough to facilitate sim-to-real transfer.

6 Conclusion

We introduce Infinigen-Sim, a tool for creating procedural generators for articulated simulation-ready assets. These assets are kinematically diverse, photorealistic, and have accurate joint configurations. Our tool also gives users fine-grained control over their assets. We use this system to create expressive generators for 5 common articulated object categories. Our experiments demonstrate that objects from these generators can improve model generalization on both perception and robot learning tasks in simulation and the real world.

We show that Infinigen-Sim assets are effective in sim-to-real transfer. We created a real-world version of the *Push Door with Handle* task using a Franka Panda robot (Fig. 5 right). For simplicity, we train imitation learning models using expert simulation trajectories. We set up an IsaacGym [47] environment for various door assets (Fig. 5 left). As we have the ground truth joint axis and origin, we rollout scripted trajectories

7 Limitations

Our work currently does not consider material physical properties such as friction or restitution. With regards to our custom joint nodes, there exist minor restrictions in the way an object’s node graph should be constructed. However, we note these restrictions do not limit the types of articulated assets that can be produced, merely the structure of the graph. We hope to continue developing our custom joint node and lift these restrictions to make our tool even more user-friendly.

For movable part segmentation, we exclusively evaluate our models on data generated using PartNet assets alone. This means certain part categories may be limited in diversity and quantity. Future work may explore the benefit of using Infinigen-Sim assets when evaluating on annotated real world images of articulated objects.

Acknowledgments

We thank Lingjie Mei for helping with modifications to the door asset. This work was partially supported by a Cisco grant and the National Science Foundation.

References

- [1] A. Raistrick, L. Mei, K. Kayan, D. Yan, Y. Zuo, B. Han, H. Wen, M. Parakh, S. Alexandropoulos, L. Lipson, Z. Ma, and J. Deng. Infinigen indoors: Photorealistic indoor scenes using procedural generation. In *Proceedings of the IEEE/CVF Conference on Computer Vision and Pattern Recognition (CVPR)*, pages 21783–21794, June 2024.
- [2] S. Tao, F. Xiang, A. Shukla, Y. Qin, X. Hinrichsen, X. Yuan, C. Bao, X. Lin, Y. Liu, T. kai Chan, Y. Gao, X. Li, T. Mu, N. Xiao, A. Gurha, Z. Huang, R. Calandra, R. Chen, S. Luo, and H. Su. Maniskill3: Gpu parallelized robotics simulation and rendering for generalizable embodied ai. *arXiv preprint arXiv:2410.00425*, 2024.
- [3] Y. Zhu, J. Wong, A. Mandlekar, R. Martín-Martín, A. Joshi, S. Nasiriany, Y. Zhu, and K. Lin. robosuite: A modular simulation framework and benchmark for robot learning. In *arXiv preprint arXiv:2009.12293*, 2020.
- [4] M. Mittal, C. Yu, Q. Yu, J. Liu, N. Rudin, D. Hoeller, J. L. Yuan, R. Singh, Y. Guo, H. Mazhar, A. Mandlekar, B. Babich, G. State, M. Hutter, and A. Garg. Orbit: A unified simulation framework for interactive robot learning environments. *IEEE Robotics and Automation Letters*, 8(6):3740–3747, 2023. doi:10.1109/LRA.2023.3270034.
- [5] M. Deitke, E. VanderBilt, A. Herrasti, L. Weihs, J. Salvador, K. Ehsani, W. Han, E. Kolve, A. Farhadi, A. Kembhavi, and R. Mottaghi. ProcTHOR: Large-Scale Embodied AI Using Procedural Generation. In *NeurIPS*, 2022. Outstanding Paper Award.
- [6] C. Li, F. Xia, R. Martín-Martín, M. Lingelbach, S. Srivastava, B. Shen, K. E. Vainio, C. Gokmen, G. Dharan, T. Jain, A. Kurenkov, K. Liu, H. Gweon, J. Wu, L. Fei-Fei, and S. Savarese. igibson 2.0: Object-centric simulation for robot learning of everyday household tasks. In A. Faust, D. Hsu, and G. Neumann, editors, *Proceedings of the 5th Conference on Robot Learning*, volume 164 of *Proceedings of Machine Learning Research*, pages 455–465. PMLR, 08–11 Nov 2022. URL <https://proceedings.mlr.press/v164/li22b.html>.
- [7] G. Authors. Genesis: A universal and generative physics engine for robotics and beyond, December 2024. URL <https://github.com/Genesis-Embodied-AI/Genesis>.
- [8] J. Lee, J. Hwangbo, L. Wellhausen, V. Koltun, and M. Hutter. Learning quadrupedal locomotion over challenging terrain. *Science Robotics*, 5(47):eabc5986, 2020. doi:10.1126/scirobotics.abc5986. URL <https://www.science.org/doi/abs/10.1126/scirobotics.abc5986>.

[9] S. Nasiriany, A. Maddukuri, L. Zhang, A. Parikh, A. Lo, A. Joshi, A. Mandlekar, and Y. Zhu. Robocasa: Large-scale simulation of everyday tasks for generalist robots. In *Robotics: Science and Systems*, 2024.

[10] Y. J. Ma, W. Liang, H. Wang, S. Wang, Y. Zhu, L. Fan, O. Bastani, and D. Jayaraman. Dreureka: Language model guided sim-to-real transfer. In *Robotics: Science and Systems (RSS)*, 2024.

[11] K. Zakka, B. Tabanpour, Q. Liao, M. Haiderbhai, S. Holt, J. Y. Luo, A. Allshire, E. Frey, K. Sreenath, L. A. Kahrs, C. Sferrazza, Y. Tassa, and P. Abbeel. Mujoco playground: An open-source framework for gpu-accelerated robot learning and sim-to-real transfer., 2025. URL https://github.com/google-deepmind/mujoco_playground.

[12] A. Wei, A. Agarwal, B. Chen, R. Bosworth, N. Pfaff, and R. Tedrake. Empirical analysis of sim-and-real cotraining of diffusion policies for planar pushing from pixels, 2025. URL <https://arxiv.org/abs/2503.22634>.

[13] J. Bjorck, F. Castañeda, N. Cherniadev, X. Da, R. Ding, L. Fan, Y. Fang, D. Fox, F. Hu, S. Huang, et al. Gr00t n1: An open foundation model for generalist humanoid robots. *arXiv preprint arXiv:2503.14734*, 2025.

[14] A. Maddukuri, Z. Jiang, L. Y. Chen, S. Nasiriany, Y. Xie, Y. Fang, W. Huang, Z. Wang, Z. Xu, N. Cherniadev, S. Reed, K. Goldberg, A. Mandlekar, L. Fan, and Y. Zhu. Sim-and-real cotraining: A simple recipe for vision-based robotic manipulation. In *Proceedings of Robotics: Science and Systems (RSS)*, Los Angeles, CA, USA, 2025.

[15] A. X. Chang, T. Funkhouser, L. Guibas, P. Hanrahan, Q. Huang, Z. Li, S. Savarese, M. Savva, S. Song, H. Su, et al. Shapenet: An information-rich 3d model repository. *arXiv preprint arXiv:1512.03012*, 2015.

[16] M. Deitke, R. Liu, M. Wallingford, H. Ngo, O. Michel, A. Kusupati, A. Fan, C. Laforte, V. Voleti, S. Y. Gadre, E. VanderBilt, A. Kembhavi, C. Vondrick, G. Gkioxari, K. Ehsani, L. Schmidt, and A. Farhadi. Objaverse-xl: A universe of 10m+ 3d objects. *arXiv preprint arXiv:2307.05663*, 2023.

[17] T. Wu, J. Zhang, X. Fu, Y. Wang, L. P. Jiawei Ren, W. Wu, L. Yang, J. Wang, C. Qian, D. Lin, and Z. Liu. Omniobject3d: Large-vocabulary 3d object dataset for realistic perception, reconstruction and generation. In *IEEE/CVF Conference on Computer Vision and Pattern Recognition (CVPR)*, 2023.

[18] F. Xiang, Y. Qin, K. Mo, Y. Xia, H. Zhu, F. Liu, M. Liu, H. Jiang, Y. Yuan, H. Wang, L. Yi, A. X. Chang, L. J. Guibas, and H. Su. SAPIEN: A simulated part-based interactive environment. In *The IEEE Conference on Computer Vision and Pattern Recognition (CVPR)*, June 2020.

[19] L. Liu, W. Xu, H. Fu, S. Qian, Q. Yu, Y. Han, and C. Lu. Akb-48: A real-world articulated object knowledge base. In *Proceedings of the IEEE/CVF Conference on Computer Vision and Pattern Recognition*, pages 14809–14818, 2022.

[20] Y. Mao, Y. Zhang, H. Jiang, A. Chang, and M. Savva. Multiscan: Scalable rgbd scanning for 3d environments with articulated objects. *Advances in neural information processing systems*, 35:9058–9071, 2022.

[21] S. Srivastava, C. Li, M. Lingelbach, R. Martín-Martín, F. Xia, K. E. Vainio, Z. Lian, C. Gokmen, S. Buch, K. Liu, S. Savarese, H. Gweon, J. Wu, and L. Fei-Fei. Behavior: Benchmark for everyday household activities in virtual, interactive, and ecological environments. In A. Faust, D. Hsu, and G. Neumann, editors, *Proceedings of the 5th Conference on Robot Learning*, volume 164 of *Proceedings of Machine Learning Research*, pages 477–490. PMLR, 08–11 Nov 2022. URL <https://proceedings.mlr.press/v164/srivastava22a.html>.

[22] C. Li, R. Zhang, J. Wong, C. Gokmen, S. Srivastava, R. Martín-Martín, C. Wang, G. Levine, M. Lingelbach, J. Sun, M. Anvari, M. Hwang, M. Sharma, A. Aydin, D. Bansal, S. Hunter, K.-Y. Kim, A. Lou, C. R. Matthews, I. Villa-Renteria, J. H. Tang, C. Tang, F. Xia, S. Savarese, H. Gweon, K. Liu, J. Wu, and L. Fei-Fei. BEHAVIOR-1k: A benchmark for embodied AI with 1,000 everyday activities and realistic simulation. In *6th Annual Conference on Robot Learning*, 2022. URL https://openreview.net/forum?id=_8DoIe8G3t.

[23] Blender Online Community. Blender - a 3d modelling and rendering package. <https://www.blender.org>, 2018. Version 4.2.

[24] K. Mo, S. Zhu, A. X. Chang, L. Yi, S. Tripathi, L. J. Guibas, and H. Su. PartNet: A large-scale benchmark for fine-grained and hierarchical part-level 3D object understanding. In *The IEEE Conference on Computer Vision and Pattern Recognition (CVPR)*, June 2019.

[25] H. Geng, H. Xu, C. Zhao, C. Xu, L. Yi, S. Huang, and H. Wang. Gapartnet: Cross-category domain-generalizable object perception and manipulation via generalizable and actionable parts. *arXiv preprint arXiv:2211.05272*, 2022.

[26] L. Liu, W. Xu, H. Fu, S. Qian, Q. Yu, Y. Han, and C. Lu. Akb-48: A real-world articulated object knowledge base. In *Proceedings of the IEEE/CVF Conference on Computer Vision and Pattern Recognition (CVPR)*, pages 14809–14818, June 2022.

[27] J. Kim, J. Kim, J. Na, and H. Joo. Parahome: Parameterizing everyday home activities towards 3d generative modeling of human-object interactions. *arXiv preprint arXiv:2401.10232*, 2024.

[28] B. Calli, A. Walsman, A. Singh, S. Srinivasa, P. Abbeel, and A. M. Dollar. Benchmarking in manipulation research: Using the yale-cmu-berkeley object and model set. *IEEE Robotics & Automation Magazine*, 22(3):36–52, Sept. 2015. ISSN 1070-9932. doi:10.1109/mra.2015.2448951. URL <http://dx.doi.org/10.1109/MRA.2015.2448951>.

[29] L. Le, J. Xie, W. Liang, H.-J. Wang, Y. Yang, Y. J. Ma, K. Vedder, A. Krishna, D. Jayaraman, and E. Eaton. Articulate-anything: Automatic modeling of articulated objects via a vision-language foundation model. *arXiv preprint arXiv:2410.13882*, 2024.

[30] X. Qiu, J. Yang, Y. Wang, Z. Chen, Y. Wang, T.-H. Wang, Z. Xian, and C. Gan. Articulate anymesh: Open-vocabulary 3d articulated objects modeling. *arXiv preprint arXiv:2502.02590*, 2025.

[31] J. Liu, M. Savva, and A. Mahdavi-Amiri. Survey on modeling of human-made articulated objects, 2025. URL <https://arxiv.org/abs/2403.14937>.

[32] Z. Jiang, C.-C. Hsu, and Y. Zhu. Ditto: Building digital twins of articulated objects from interaction. In *Conference on Computer Vision and Pattern Recognition (CVPR)*, 2022.

[33] Z. Mandi, Y. Weng, D. Bauer, and S. Song. Real2code: Reconstruct articulated objects via code generation. *arXiv preprint arXiv:2406.08474*, 2024.

[34] J. Liu, A. Mahdavi-Amiri, and M. Savva. Paris: Part-level reconstruction and motion analysis for articulated objects. In *Proceedings of the IEEE/CVF International Conference on Computer Vision*, pages 352–363, 2023.

[35] Z. Chen, A. Walsman, M. Memmel, K. Mo, A. Fang, K. Vemuri, A. Wu, D. Fox, and A. Gupta. Urdformer: A pipeline for constructing articulated simulation environments from real-world images. *arXiv preprint arXiv:2405.11656*, 2024.

[36] C.-C. Hsu, Z. Jiang, and Y. Zhu. Ditto in the house: Building articulation models of indoor scenes through interactive perception. In *IEEE International Conference on Robotics and Automation (ICRA)*, 2023.

[37] Y. Weng, B. Wen, J. Tremblay, V. Blukis, D. Fox, L. Guibas, and S. Birchfield. Neural implicit representation for building digital twins of unknown articulated objects. In *CVPR*, 2024.

[38] A. Raistrick, L. Lipson, Z. Ma, L. Mei, M. Wang, Y. Zuo, K. Kayan, H. Wen, B. Han, Y. Wang, A. Newell, H. Law, A. Goyal, K. Yang, and J. Deng. Infinite photorealistic worlds using procedural generation. In *Proceedings of the IEEE/CVF Conference on Computer Vision and Pattern Recognition*, pages 12630–12641, 2023.

[39] Y. I. H. Parish and P. Müller. Procedural modeling of cities. In *Proceedings of the 28th Annual Conference on Computer Graphics and Interactive Techniques*, SIGGRAPH '01, page 301–308, New York, NY, USA, 2001. Association for Computing Machinery. ISBN 158113374X. doi:10.1145/383259.383292. URL <https://doi.org/10.1145/383259.383292>.

[40] C. Eppner, A. Murali, C. Garrett, R. O’Flaherty, T. Hermans, W. Yang, and D. Fox. `scene_synthetizer`: A python library for procedural scene generation in robot manipulation. *Journal of Open Source Software*, 2024.

[41] J. Lei, C. Deng, W. B. Shen, L. J. Guibas, and K. Daniilidis. Nap: Neural 3d articulated object prior. In A. Oh, T. Naumann, A. Globerson, K. Saenko, M. Hardt, and S. Levine, editors, *Advances in Neural Information Processing Systems*, volume 36, pages 31878–31894. Curran Associates, Inc., 2023. URL https://proceedings.neurips.cc/paper_files/paper/2023/file/655846cc914cb7ff977a1ada40866441-Paper-Conference.pdf.

[42] J. Liu, H. I. I. Tam, A. Mahdavi-Amiri, and M. Savva. Cage: Controllable articulation generation. In *Proceedings of the IEEE/CVF Conference on Computer Vision and Pattern Recognition*, pages 17880–17889, 2024.

[43] X. Wei, M. Liu, Z. Ling, and H. Su. Approximate convex decomposition for 3d meshes with collision-aware concavity and tree search. *ACM Transactions on Graphics (TOG)*, 41(4):1–18, 2022.

[44] R. Wang, A. Gadi Patil, F. Yu, and H. Zhang. Active coarse-to-fine segmentation of moveable parts from real images. In *Computer Vision – ECCV 2024: 18th European Conference, Milan, Italy, September 29–October 4, 2024, Proceedings, Part XXXIV*, page 111–127, Berlin, Heidelberg, 2024. Springer-Verlag. ISBN 978-3-031-72753-5. doi:10.1007/978-3-031-72754-2_7. URL https://doi.org/10.1007/978-3-031-72754-2_7.

[45] Y. Li, S. Xie, X. Chen, P. Dollar, K. He, and R. Girshick. Benchmarking detection transfer learning with vision transformers, 2021. URL <https://arxiv.org/abs/2111.11429>.

[46] J. Schulman, F. Wolski, P. Dhariwal, A. Radford, and O. Klimov. Proximal policy optimization algorithms. *arXiv preprint arXiv:1707.06347*, 2017.

[47] V. Makoviychuk, L. Wawrzyniak, Y. Guo, M. Lu, K. Storey, M. Macklin, D. Hoeller, N. Rudin, A. Allshire, A. Handa, and G. State. Isaac gym: High performance gpu-based physics simulation for robot learning, 2021.

[48] T. Z. Zhao, V. Kumar, S. Levine, and C. Finn. Learning fine-grained bimanual manipulation with low-cost hardware. *arXiv preprint arXiv:2304.13705*, 2023.

Appendix

A.1 Example Procedural Assets

In this section, we present several examples of assets created using our custom generators. The distributions shown reflect the default settings but can be customized as needed.

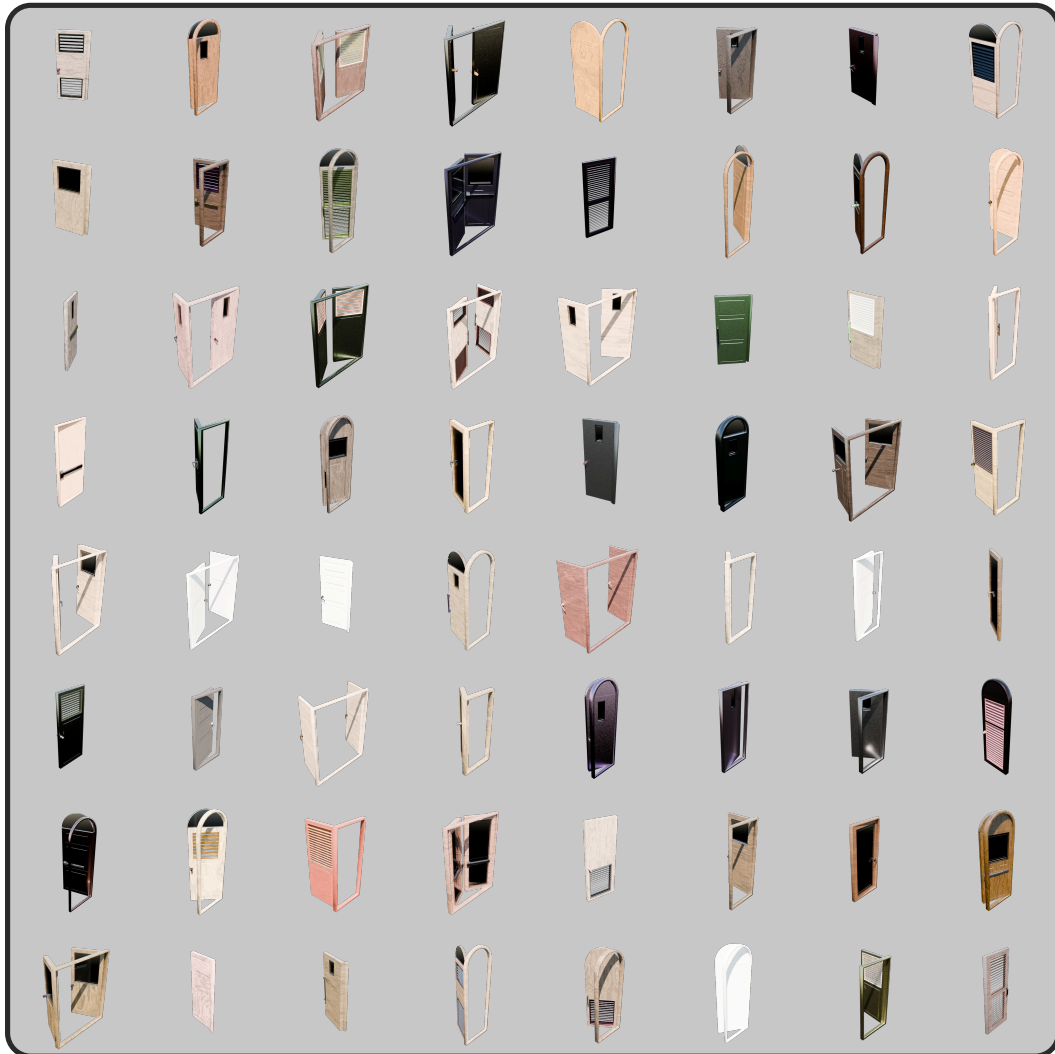


Figure 6: Procedurally generated articulated doors with handles.

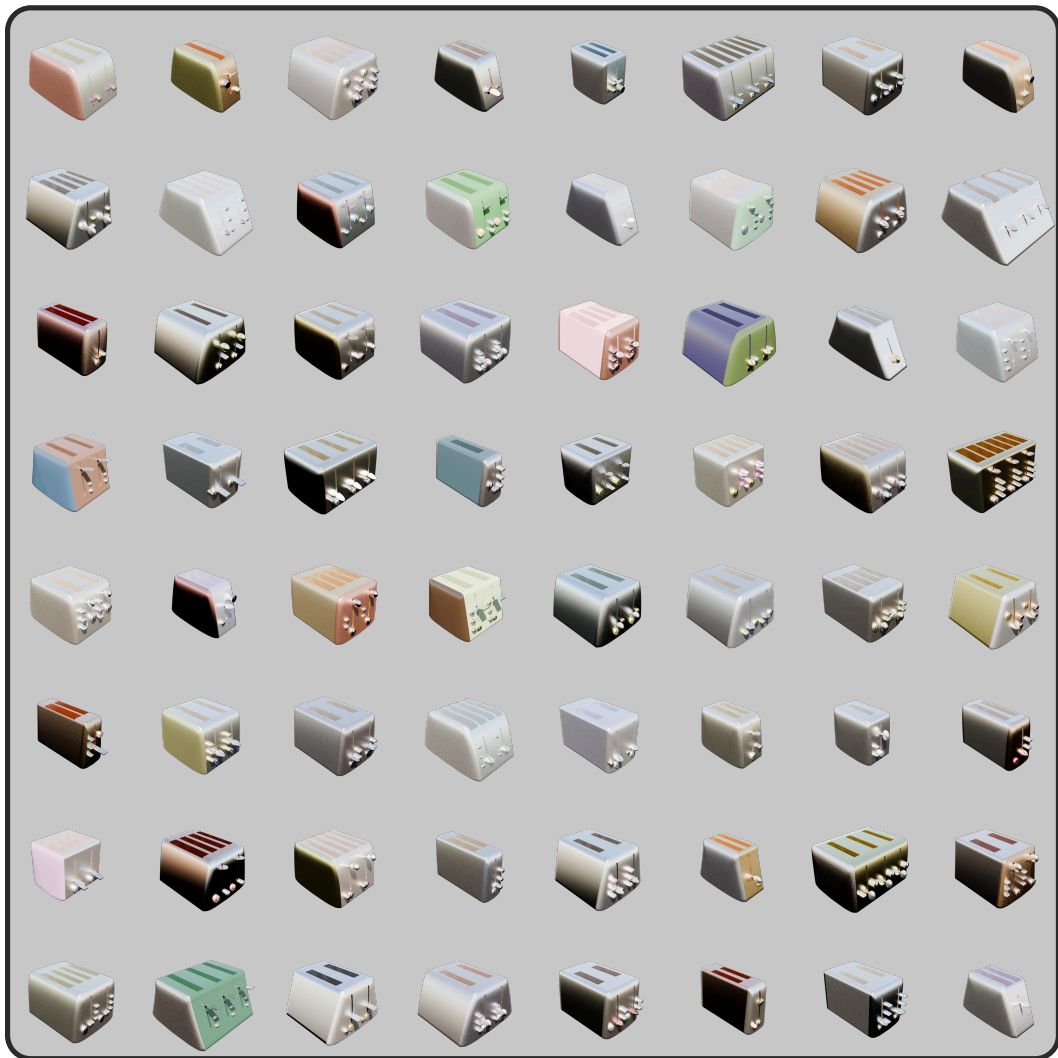


Figure 7: Procedurally generated articulated toasters with levers, buttons, and knobs.



Figure 8: Procedurally generated articulated refrigerators with internals/external drawers and shelves.

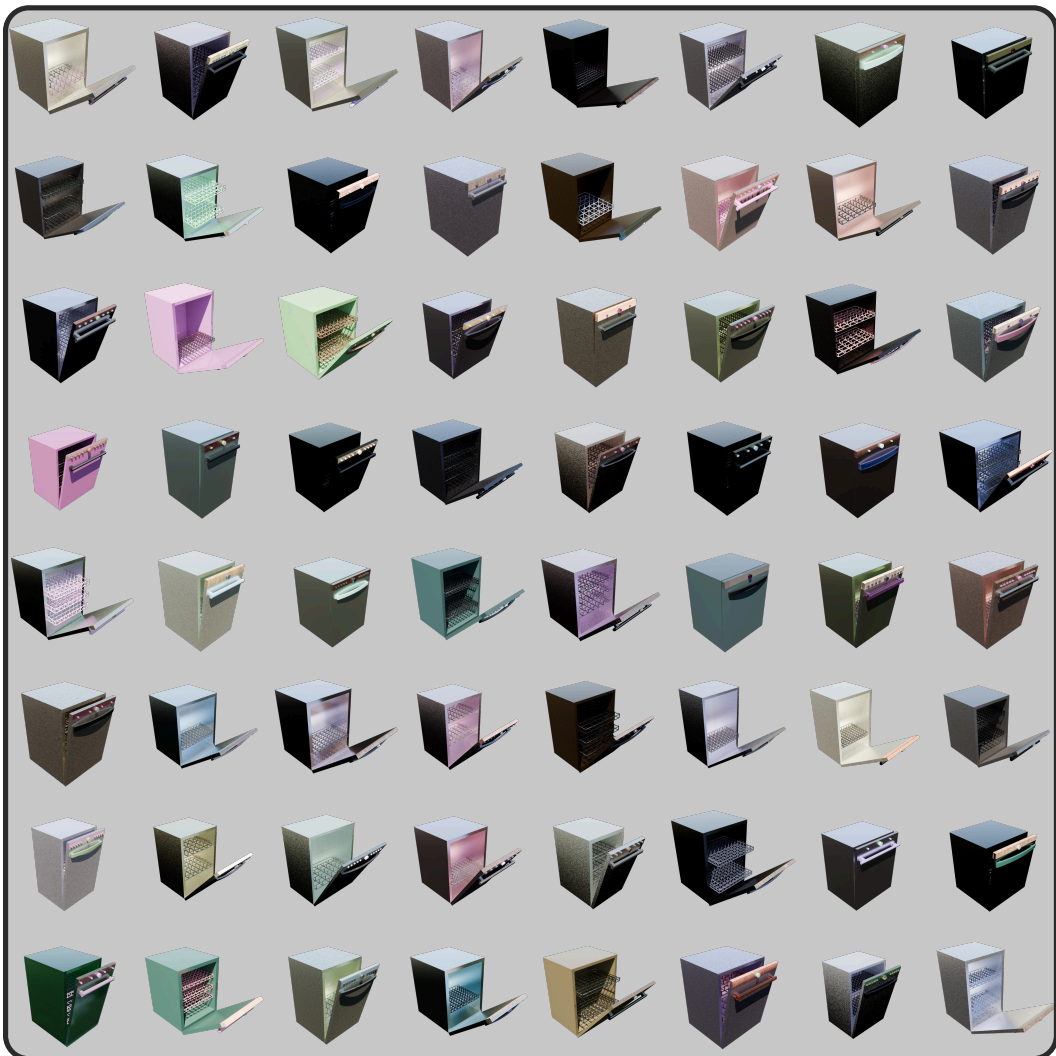


Figure 9: Procedurally generated articulated dishwashers with handles, racks, buttons, and knobs.

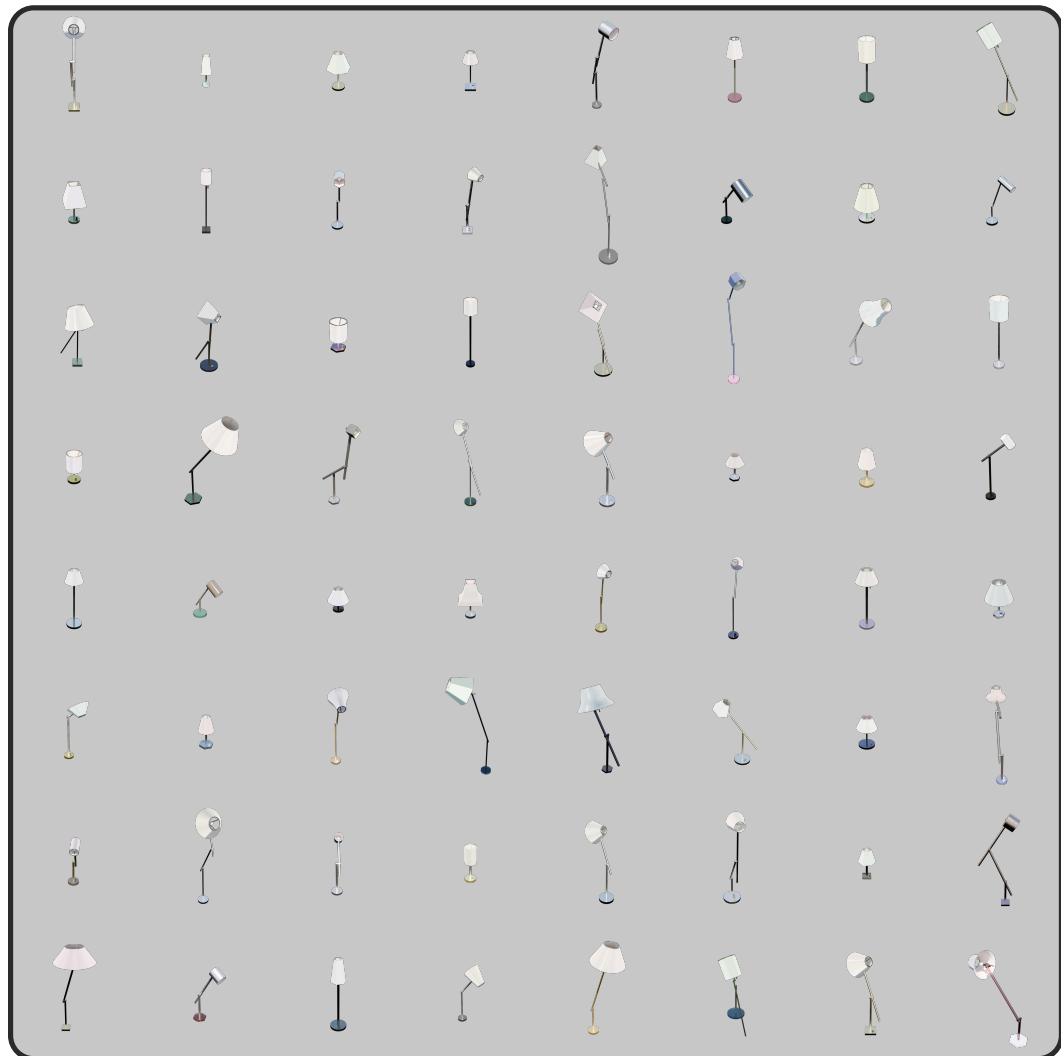


Figure 10: Procedurally generated articulated lamps with many different types of switches.

A.2 Example Articulations

In this section, we showcase minimal examples of how our custom joint nodes can be used to create different types of articulations within Blender. These articulated assets directly translate to simulation using our native exporters for the URDF, USD, and MJCF file types.

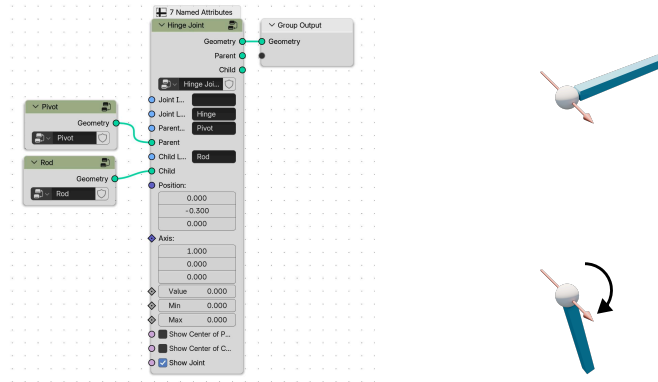


Figure 11: **Simple Revolute Joint**: Demonstrates a rod rotating about a pivot point. Our nodes include togglable debugging features, such as axis visualization, to assist users in verifying joints.

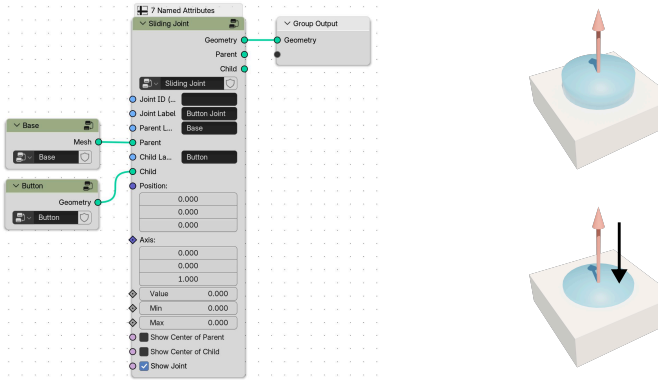


Figure 12: **Simple Prismatic Joint**: Demonstrates an articulated button using our custom joint node.

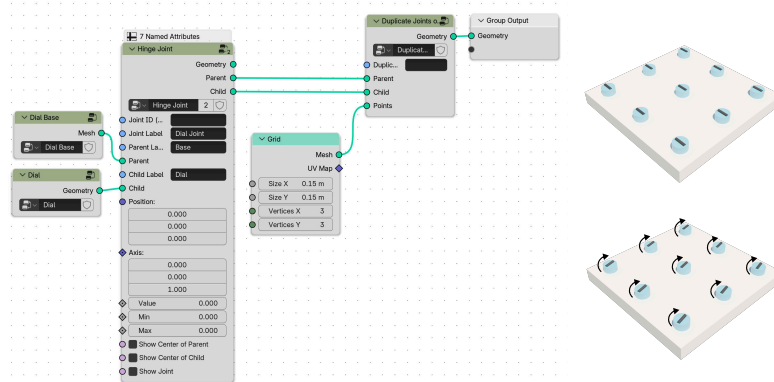


Figure 13: **Duplicating Jointed Bodies**: Demonstrates duplication of multiple articulated knobs. Instead of manually defining a joint for each knob, this node automatically replicates the articulated body at a set of points (a grid in this example).

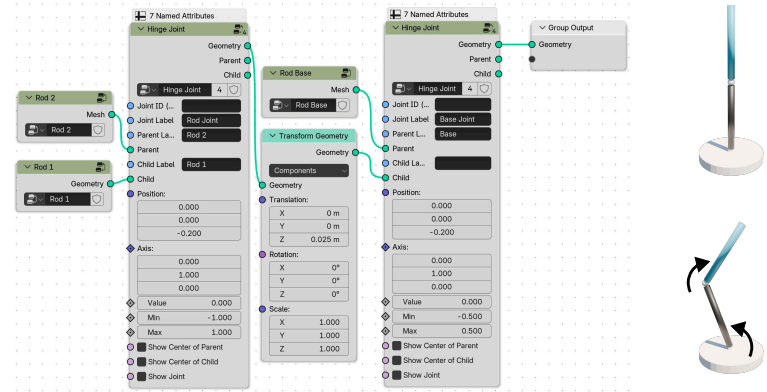


Figure 14: **Connecting Multiple Jointed Bodies:** Demonstrates connecting multiple bodies together. We first joint the two rods together, followed by jointing the combined body with the base.

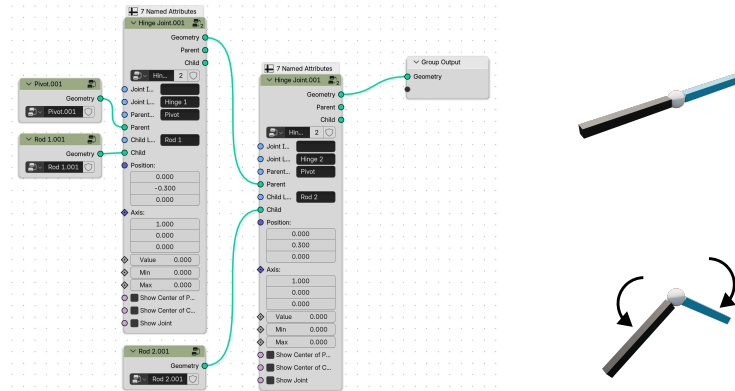


Figure 15: **Jointing to the Same Body:** Demonstrates jointing two rods to the same sphere. First, one rod is jointed to the sphere to form a body. Then, the second rod is jointed to this body by attaching it to the top-most parent object (i.e. the sphere).

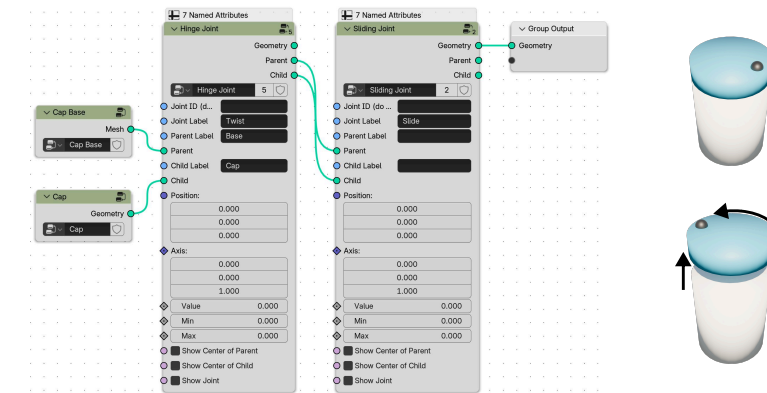


Figure 16: **Multi-Jointed Bodies:** Demonstrates a multi-jointed articulated cap. Combining a hinge and slide joint can achieve a screw joint commonly used for assets such as water bottles.

A.3 List of Interpretable Degrees of Freedom

Articulated Object	DOF	Interpretable Parameters
Toaster	14	Dimension of Lever handle, Slot Width, Slot Length, Slot Depth, Toaster Length, Knob Vertical Location, Knob Horizontal Location, Knob Size, Circular Button Size, Square Button Width, Inter-Button Distances, Button Horizontal Offset, Button Vertical Offset, Protrusion parameter
Fridge	32	Size, Wall Thickness, Body Outer Roundness, Body Inner Roundness, Door Handle Margin, Door Shelf Size, Door Shelf Thickness, Door Shelf Num, Door Shelf Margin, Door Handle Top Size, Door Handle Top Thickness, Door Handle Top Roundness, Door Handle Support Size, Door Handle Support Margin, Door Left Margin, Door Right Margin, Door Upper Margin, Door Lower Margin, Shelf Margin, Shelf Thickness, Shelf Board Margin, Drawer Height, Drawer Wall Thickness, Drawer Handle Margin, Drawer Handle Top Size, Drawer Handle Top Thickness, Drawer Handle Top Roundness, Drawer Handle Support Size, Drawer Handle Support Margin, Drawer Body Roundness, Drawer Slide Roundness, Drawer Inner Roundness
Dishwasher	13	Depth, Width, Height, Door Thickness, Rack Radius, Rack Height, Rack Depth, Handle Radius, Handle Position, Number of Racks, Density of Supports in Rack, Button Position, Handle Curvature
Lamp	29	Pull String Radius, Pull String Base Height, Pull String Length, Button Base Size, Button Size, Button Height, Twist Button Base Size, Twist Button Size, Twist Button Height, Twist Button Twister height, Switch Base Size, Switch Size, Switch Curvature, Button X-Location, Length of Bar 1, Location of Bar 2 joint on Bar 1, Length of Bar 2, Location of Bar 3 joint on Bar 2, Radius, Height, Radius of Base, Base Height, Number of Sides on Base, Shade Height, Rack Height, Top Radius, Bottom Radius, Rack Thickness, Number of Sides on Shade
Door	39	Width, Height, Depth, Panel margin, Bevel Width, Shrink Width, Door Frame Width, Handle Height, Push Bar Length, Push Bar Thickness, Push Bar Aspect Ratio, Push Bar Height Ratio, Push Bar Length Ratio, Push Bar End Length Ratio, Push Bar End Height Ratio, Push Bar Overall Z-Offset, Knob Radius, Knob Base Radius, Knob Middle Radius, Knob Central Radius, Knob Depth, Knob Middle Depth, Lever Radius, Lever Middle Radius, Lever Depth, Lever Middle Depth, Lever Length, Lever Type, Pull Handle Size, Pull Handle Depth, Pull Handle Width, Pull Handle Extension, Pull Handle Bevel Width, Pull Handle Pull Radius, Pull Handle Bevel Side Length, Louver Width, Louver Margin, Louver Size, Louver Angle

Table 3: Toaster, refrigerator, dishwasher, lamp, and door generators with interpretable degrees of freedom and named parameters

A.4 Experiment Setup of Movable Part Segmentation

In order to run the experiments as described in Sec. 5.1, we first generate images using and ground truth labels and segmentations for both the PartNet-Mobility and Infinigen-Sim assets. Each image is of size 1024×1024 to ensure that smaller movable parts are visible. Similar to Xiang et al. [18], images are taken from a camera positioned randomly on the upper hemisphere of the asset with the scene having ambient lighting and fixed directional lighting. We also randomly sample the field of view. Finally, we randomize the joint values so that the same asset appears in different poses across images. For assets such as dishwashers where interior racks may intersect with exterior bodies, we sample joint values within a range to try to avoid this. All images are rendered using ray-tracing with Maniskill3 [2].

In order to curate the evaluation dataset for the movable part segmentation experiments, we first randomly sample PartNet-Mobility assets such that there exists at least one asset for each considered movable part. To ensure fairness and valid evaluation, we then remove invalid assets from the evaluation set based on the following criteria:

1. Asset includes parts that should be movable but are not (i.e. the mesh of a button is present, but the button is not articulated).
2. Asset contains invalid geometries such as holes or protruding triangles.
3. Asset contains incorrect face normals, resulting in transparent parts.

We then subsample the evaluation dataset such that we have 25% of assets from each model category, ensuring at least one asset remains for each movable part. Both invalid and subsampled assets are moved back to the PartNet-Mobility training dataset.

During training, we use the following hyperparameters to train our Mask R-CNN model:

Hyperparameter	Value
Learning Rate	1e-4
Weight Decay	1e-5
Evaluation Mask Treshold	0.5
Batch Size	4
Optimizer	Adam
Epochs	10

Table 4: Mask R-CNN Training Hyperparameters

A.5 Overall Results of Movable Part Segmentation

In this section, we provide the overall results for the movable part segmentation experiments. We observe an overall increase in performance when training our Mask R-CNN model on a combination of both PartNet-Mobility and Infinigen-Sim assets. We attribute this boost in performance to the increase diversity introduced when training on Infinigen-Sim assets. This diversity likely allows the model to be more robust to unseen objects.

Dataset	mAP	mAP_{50}	mAP_{75}	mAP_{small}	mAP_{medium}	mAP_{large}
Partx1	48.23	63.22	50.14	9.09	30.03	62.46
Partx2	48.46	63.42	50.29	9.37	29.57	62.93
Partx1+Inf	50.13	64.92	51.97	9.92	32.10	62.27

Table 5: Movable part segmentation mAP scores for all experiments averaged across three seeds. We train each model for 50 epochs.

A.6 Experiment Setup of RL Generalization

We train RL agents on *Push Down Toaster Lever*, *Push Door with Handle*, and *Open Fridge Door* to show that Infinigen-Sim assets create a better asset distribution for generalizable robot policies on new instances. In all our experiments, we only use assets from PartNet-Mobility [18] for evaluation. For fair comparison, all policies are trained with 64 GPU-based parallel environment with instances sampled from the training distributions, i.e., PartNet only v.s. PartNet + Infinigen-Sim. In Figure 4, we plot the learning curve of evaluation success rate averaged over 4 seeds.

Push Down Toaster Lever. The robot is tasked with pushing down the lever of the toaster. Only toasters with a single lever are considered for this task. We evaluate on 5 unseen PartNet toasters and compare RL policies where one is trained on the remaining 8 PartNet toasters while the other is trained on 8 PartNet and 14 Infinigen-Sim toasters.

In RL training, we use the reward to encourage the fingertip to approach the lever, to push down the lever, and to penalize on the action scale. The task is considered as a success if the lever is pushed more than 50% of its joint range. The policy takes an on-the-shoulder, third-person RGB image (Figure 4) + fingertip pose as inputs and outputs a 6-dim delta pose change. The action commands the Operation Space Controller (OSC).

Push Door with Handle. The robot needs to push the door open by first rotating the door handle clockwise by more than 40 degrees. Only single doors with a lever handle are considered for this task. We evaluate on 3 PartNet doors with handles and compare RL policies where one is trained on the remaining 3 PartNet doors while the other is trained on 3 PartNet and 44 Infinigen-Sim doors.

In RL training, we use the reward to encourage the fingertip to approach the handle, to rotate the handle, and to push the door to open. We consider a trial as a success if the door is opened by at least 15 degrees. The policy takes an on-the-shoulder, third-person RGB image (Figure 4) + fingertip pose as inputs and outputs a 6-dim delta pose change. The action commands the Operation Space Controller (OSC).

Open Fridge Door. The robot is tasked with grasping the handle and opening the fridge door. Only refrigerators with a single door are considered for this task. We evaluate on 5 PartNet fridges and compare RL policies where one is trained on the remaining 5 PartNet fridges while the other is trained on 5 PartNet and 44 Infinigen-Sim fridges.

In RL training, we use the reward to encourage the fingertip to approach the door and to open the door. We consider the trial as a success if the door is opened by at least 15 degrees. The policy takes an on-the-shoulder, third-person RGB image (Figure 4) + fingertip pose as inputs and outputs a 6-dim delta pose change. The action commands the Operation Space Controller (OSC). Noticing that, we do not require to use the handle to successfully open the door.

In our results (Fig. 4), we show that policies trained with both Infinigen-Sim and PartNet assets can have a better generalization performance and more stable learning curve than the policy trained with PartNet assets only. However, the current success rate is still low to solve the tasks. We leave this as future work to train robust and better policies for these tasks with potentially more Infinigen-Sim assets.

A.7 Experiment Setup of Sim-to-Real Transfer

We apply a procedural approach to generate expert trajectories. Giving handle assets, we pre-sample candidate pre-grasps and grasp poses according to the handle position and its bounding box. Moreover, we use CuRobo to solve IK of pre-grasp poses as initialization of trajectories and use OSC to generate a cartesian linear trajectory to the grasp pose. After finger closure, we generate a circular cartesian motion to rotate the handle along the handle joint axis. The axis direction and its origin is known given the asset annotations. After the rotation is more than 45 degrees, we generate door opening circular motion, given the door joint position and origin. As this procedural pipeline may not work for some grasp poses and door assets, we filter the trajectories with success criteria and

use the curated trajectories as the imitation learning dataset. All our trajectories are generated and rendered in IsaacGym [47], with its default rendering engine.

The imitation learning policy outputs target 6-dof poses in the robot base and 1-dim for gripper action, instead of delta motion [48]. Here, the input only consists the on-the-shoulder, third-person view RGB image and its fingertip pose (Fig. 5). The training configuration follows [48]. On a real Franka robot, we use DEOXYS to command the real robot with an OSC controller for the absolute target pose. We set a relative stiff PD value as the task requires certain strength to solve.